Supporting Information for:

Upcycling Waste PET into Functional Multiblock Copolymers through Controlled Macromolecular Design

Shelby Watson-Sanders,[1] Alison Biery,[1] Karina Guerrero,[1] Nicholas J. Galan,[2] Tomonori Saito,[2] Brian K. Long,[1] Mark D. Dadmun[1,*]
[1]Department of Chemistry, University of Tennessee, Knoxville, TN 37996

[2]Oak Ridge National Laboratory, Oak Ridge, TN
* Corresponding Author (Dad@utk.edu)

Table of Contents

Methods

Depolymerization of PET

The catalyst was prepared using the same methods described by Jehanno et al.[1] The salt catalyst was created by mixing Triazabicyclodecene (TBD) and Methanesulfonic acid (MSA) at a 1:1 molar ratio, heating the mixture to 80 °C for 20 minutes or until it solidified. The resulting product was a transparent, homogeneous solid. In this form, the strongly basic TBD is converted into its conjugate acid and used as a neutral ionic catalyst during glycolysis rather than as a free base. Ethylene Glycol (EG), the TBD:MSA catalyst, PET (with a molar ratio of 20:0.5:1), and a stir bar were all placed in a 20 mL reaction vial inside a glovebox, sealed with septa, and then transferred outside the glovebox into a 180 °C oil bath, as shown in **Scheme S1**. Prior research indicates that this reaction typically completes within 2 hours at 180 °C. After the designated reaction time, the vials were removed from the oil bath. The EG and depolymerization products soluble in EG were promptly decanted while hot from the vials. The insoluble solid PET was washed three times with water by suspending it in 20 mL of water and stirring with a stir bar for 15 minutes each time. After the third wash and decanting, the vial containing the water-washed, EG-insoluble materials was placed on a 70 °C hotplate overnight to evaporate any residual water.

Scheme S1 Depolymerization of Polyethylene Terephthalate (PET) via glycolysis using organo salt catalyst (TBD:MSA)

BHET polymerization via excess diisocyanate coupling

A 50 mL round-bottom flask was charged with dihydroxy-capped bis(2-hydroxyethyl) terephthalate (BHET, 1g) and a stir bar, and then sealed with a septum. The round-bottom flask

was flushed with N_2 gas, and then 10 mL of tetrachloroethane (TCE) was added. The vessel was placed in a 130 °C oil bath on a 250 RPM stir plate to allow the BHET to dissolve in the TCE. Once the BHET was fully dissolved, 1,6-diisocyanatohexane (HDI) was added in a 1:1 molar ratio of isocyanate to hydroxyl end groups (HDI/PEO), as shown in **Scheme S2**. Aliquots were taken at 0.25 hour, 0.5 hour, 1 hour, and 2 hours. After the reaction ran for 18 hours, it was quenched with a 250 mL mixture of 1:10 isopropyl alcohol (IPA):hexane. BHET is insoluble in hexane, allowing for the polymer to precipitate. IPA was utilized to terminate the reaction by reacting with any residual isocyanate groups.

Scheme S2 Polymerization of bis(2-hydroxyethyl) terephthalate (BHET) with 1,6-diisocyanatohexane (HDI)

PEO repolymerization via excess diisocyanate coupling

A 50 mL round-bottom flask was charged with dihydroxy-capped Polyethylene oxide (PEO, 1g, 4 kDa M_n, 1.06 Đ) and a stir bar, and then sealed with a septum. The round-bottom flask was flushed with N_2 gas, and then 10 mL of tetrachloroethane (TCE) was added. The vessel was placed in a 130 °C oil bath on a 250 RPM stir plate to allow the PEO to dissolve in the TCE. Once the PEO was fully dissolved, 1,6-diisocyanatohexane (HDI) was added in a 2:1 molar ratio of isocyanate to hydroxyl end groups (HDI/PEO), as shown in **Scheme S3**. After the reaction ran for a total of 24 hours, it was quenched with a 250 mL mixture of 1:10 isopropyl alcohol (IPA):hexane. PEO is insoluble in hexane, allowing for the polymer to precipitate. IPA was utilized to terminate the reaction by reacting with any residual isocyanate groups.

Scheme S3 Polymerization of Polyethylene oxide (PEO) oligomer with 1,6-diisocyanatohexane (HDI)

BHET-PEO polymerization via diisocyanate coupling

A 50 mL round-bottom flask was charged with dihydroxy-capped BHET (1g) and a stir bar, and then sealed with a septum. The round-bottom flask was flushed with N_2 gas, and then 10 mL of TCE was added. The vessel was placed in a 130 °C oil bath on a 250 RPM stir plate to allow the BHET to dissolve in the TCE. Once the BHET was fully dissolved, HDI was added in a 2.05:1 molar ratio of isocyanate to hydroxyl end groups (HDI/BHET), as shown in **Scheme S4**. A 10 wt% mixture of PEO (4 kDa, 1.06 Đ) in TCE flushed with N_2 gas was made. Once the diisocyanate coupling reaction of BHET had run for 10 minutes, PEO dissolved in TCE was added in a 1:1 molar ratio of PEO hydroxyl groups to BHET hydroxyl groups, as shown in **Scheme S4**. Aliquots were taken at 0.25 hour, 0.5 hour, 1 hour, and 2 hours. After the reaction ran for a total of 18 hours, it was quenched with a 250 mL mixture of 1:10 IPA:hexane. Neither BHET nor PEO is soluble in hexane, allowing for the polymer to precipitate. IPA was utilized to terminate the reaction by reacting with any residual isocyanate groups.

Scheme S4 End capping of BHET with 1,6-diisocyanatohexane (HDI) and then polymerization of Polyethylene oxide (PEO) oligomer with diisocyanate-BHET monomer.

Multiblock Copolymer (MBCP) PET-PEO: 24 hour End-Capping

Prior to HDI-mediated coupling, the depolymerized PET oligomers were purified to remove residual TBD:MSA catalyst and ethylene glycol. The solid glycolysis product was dissolved in HFIP and precipitated into methanol, collected, and dried; this HFIP/MeOH

dissolution-precipitation protocol was repeated three times. These repeated precipitations remove low-molecular-weight species, including the TBD:MSA salt and residual EG, yielding a purified telechelic PET oligomer fraction that was used as the feedstock for subsequent PET-PEO multiblock synthesis.

A 50 mL round-bottom flask was charged with dihydroxy-capped PET oligomers (1g, 5.7 kDa M_n, 1.53 Đ) and a stir bar, and then sealed with a septum. The round-bottom flask was flushed with N_2 gas, and then 10 mL of TCE was added. The vessel was placed in a 140 °C oil bath on a 250 RPM stir plate to allow the PET to dissolve in the TCE. Once the PET was fully dissolved, the oil bath temperature was decreased to 130 °C, and HDI was added in a 2.05:1 molar ratio of isocyanate to hydroxyl end groups (HDI/PET), as shown in **Scheme S6**. A 10 wt% mixture of PEO (4 kDa, 1.06 Đ) in TCE flushed with N_2 gas was made. Once the diisocyanate coupling reaction of PET had run for 24 hours, PEO dissolved in TCE was added in a 1:1 molar ratio of PEO hydroxyl groups to PET hydroxyl groups, as shown in **Scheme S6**. After 46 hours (22 hours after PEO addition), the reaction was quenched with a 250 mL mixture of 1:10 IPA:hexane. Neither PET nor PEO is soluble in hexane, allowing for the polymer to precipitate. IPA was utilized to terminate the reaction by reacting with any residual isocyanate groups. For PET-PEO multiblock synthesis, PET oligomers, HDI, and PEO were reacted in a single pot without isolating the PET-HDI intermediate. HDI was added in a 2.05:1 molar ratio relative to PET hydroxyl groups to provide sufficient isocyanate functionality for both PET end-capping and subsequent coupling to PEO. After the desired total reaction time, the PET/PEO reaction mixture was quenched with isopropanol (IPA) to react with any residual isocyanate groups, thereby terminating chain growth and preventing further formation of PEO-HDI species.

Scheme S5 End capping of PET oligomer with 1,6-diisocyanatohexane (HDI) and then polymerization of PEO oligomer with diisocyanate-PET macromonomer.

FTIR

Fourier transform infrared (FT-IR) spectra were collected using a Thermo Scientific FT-IR spectrometer operating in absorbance mode. Background spectra were acquired prior to each set of measurements by averaging 32 scans, and sample spectra were collected by averaging 64 scans to improve the signal-to-noise ratio.

Nuclear Magnetic Resonance (NMR)

In the NMR analysis, the PET oligomers, PEO oligomers, BHET, rPEO, PEO-BHET, PET-PEO, Polycarbonate (PC), and depolymerized PC (30-60 mg) were dissolved in HFIP (1 mL). The sample:HFIP mixture was agitated for five days before 100 microliters of the mixture were mixed with 600 microliters of $CDCl_3$. The NMR data were obtained using a JEOL 400 YH NMR at 35 °C for 160 scans to ensure the sample did not precipitate from solution. The number-average molar masses (M_n) of the depolymerized PET products were determined using the analysis outlined by Falkenstein.[2]

Virgin and depolymerized PET show peaks at 8.0 ppm (4H, terephthalic protons), 4.65 ppm (4H, methylene protons), and 4.01 ppm (2H, methylene protons on the alpha carbon to the hydroxyl end group). Isocyanate-coupled PEO (rPEO) has peaks at 3.52 ppm (4H, PEO methylene protons), 1.50 ppm, 1.29 ppm, 3.18 ppm (12H, HDI methylene protons), 6.76 ppm (2H, urethane proton), 4.77 ppm and 1.19 ppm (7H, isopropoxy end group protons). PEO-BHET has peaks at 3.52 ppm (4H, PEO methylene protons), 1.50 ppm, 1.29 ppm, 3.18 ppm (12H, HDI methylene protons), 6.76 ppm (2H, urethane proton), 4.77 ppm and 1.19 ppm (7H, isopropoxy end group

protons), along with peaks at 8.0 ppm (4H, terephthalic protons), and 4.65 ppm (4H, methylene protons). PEO-PET displays peaks at 3.52 ppm (4H, PEO methylene protons), 1.50 ppm, 1.29 ppm, 3.18 ppm (12H, HDI methylene protons), 6.76 ppm (2H, urethane proton), 4.77 ppm and 1.19 ppm (7H, isopropoxy end group protons), as well as peaks at 8.0 ppm (4H, terephthalic protons), and 4.65 ppm (4H, methylene protons). PC and depolymerized PC have peaks at 7.05-7.25 (8H, aromatic protons) and at 1.72 (6H, methylene protons).

Average Hydroxyl Groups per chain

To determine the amount of HDI needed for polymerizations utilizing PET oligomers, the average number of hydroxyl end groups per chain was calculated. Determining the M_n value from NMR requires knowing the amount of hydroxyl end groups. However, during glycolysis, the number of hydroxyl end groups per oligomer can vary between 1 and 2. As previous work in our group[3] shows, when M_n values from SEC and NMR are compared, the average number of hydroxyl end groups per chain can be found when those values (M_n from NMR and SEC) are the same. **Figure S1** illustrates how the number-average molar mass (M_n) calculated from ^{1}H NMR depends on the assumed average number of hydroxyl end groups per PET chain. When Mn is calculated from NMR, a specific number of end groups must be assumed; varying this assumption between 1 and 2 hydroxyl groups per chain yields a continuous range of possible Mn values, shown as the solid line. This relationship reflects the inherent ambiguity of NMR-based Mn determination in telechelic oligomers, where end-group functionality cannot be independently verified solely from integration. The experimentally measured Mn obtained from GPC is overlaid as a discrete data point. By locating where the GPC-derived Mn intersects the NMR-based trend, the average number of hydroxyl end groups per chain can be inferred. This intersection, therefore, provides an independent estimate of end-group functionality, anchoring the NMR calculation to an absolute

molar mass measurement. This approach enables quantitative determination of hydroxyl end-group density in depolymerized and repolymerized PET samples and was applied consistently throughout this work.

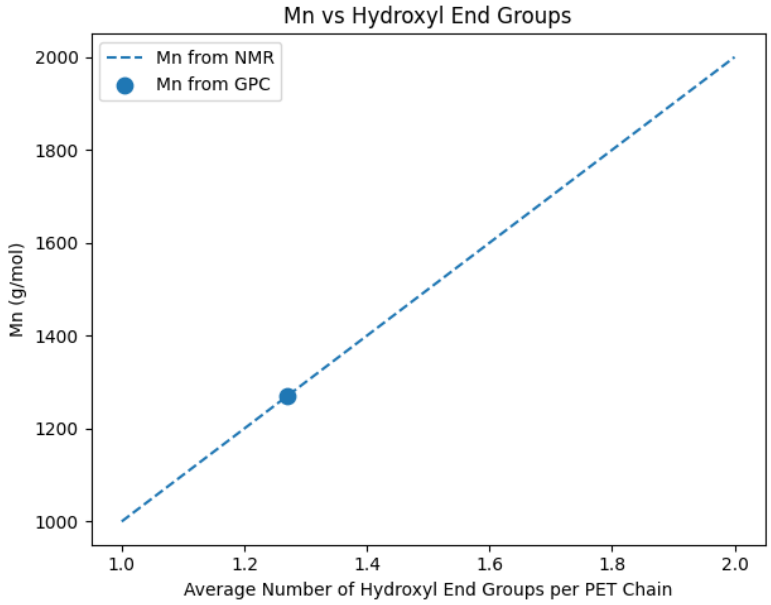

Sample	Hydroxyl End Groups	Mn (g/mol)
Mn from NMR	1.00	1000
Mn from NMR	1.10	1100
Mn from NMR	1.20	1200
Mn from NMR	1.30	1300
Mn from NMR	1.40	1400
Mn from NMR	1.50	1500
Mn from NMR	1.60	1600
Mn from NMR	1.70	1700
Mn from NMR	1.80	1800
Mn from NMR	1.90	1900
Mn from NMR	2.00	2000
Mn from GPC	1.27	1270

Figure S1. Relationship between number-average molar mass (M_n) calculated from ^{1}H NMR and the assumed average number of hydroxyl end groups per PET chain. The solid line represents Mn values calculated by NMR, assuming between one and two hydroxyl end groups per chain. The discrete point corresponds to the experimentally measured M_n obtained from GPC. The intersection of the GPC-derived M_n with the NMR trend provides an estimate of the average hydroxyl end-group density per chain, enabling quantitative determination of end-group functionality in depolymerized and repolymerized PET samples.

DOSY (Diffusion Ordered Spectroscopy)

Polymers were analyzed by DOSY NMR using a Dbppste sequence with convection compensation. Samples were temperature-regulated (35 °C), resonance-locked, tuned, and shimmed. Parameters included nt (multiple of 16), gzlvl1 (500-30,000; ≤30 points), and del (0.05-0.1, 0.01 steps). Two spectra were recorded at each del; the final setting yielded ~10% intensity in

the second spectrum. Diffusion gradient length was 4.0 ms. Data were processed for diffusion coefficients and checked via standard software.

Polycarbonate Depolymerization

A 25 mL round-bottom flask was charged with 1 g of PC, 10 mL of THF, and a stir bar. The flask, equipped with a condenser, was placed in a 70 °C oil bath to reflux and dissolve the PC. Once fully dissolved, either EG or BPA was added, followed quickly by TEA at a molar ratio of 1:1:0.5 relative to PC:EG/BPA:TEA, as shown in **Scheme S7.** Aliquots were collected every 2 minutes for up to 12 minutes for EG and up to 24 minutes for BPA. These samples were analyzed using GPC with THF to determine molar masses, and NMR was employed to assess the number of phenol end groups.

Scheme S6 Homogeneous depolymerization of Polycarbonate in THF with ethylene glycol or bisphenol-A

BPA-PEO polymerization via diisocyanate coupling

A 50 mL round-bottom flask was charged with diphenol-capped BPA (1g) and a stir bar, and then sealed with a septum. The round-bottom flask was flushed with N_2 gas, and then 10 mL of TCE was added. The vessel was placed in a 130 °C oil bath on a 250 RPM stir plate to allow the BPA to dissolve in the THF. Once the BPA was fully dissolved, HDI was added in a 2.05:1 molar ratio of isocyanate to phenol end groups (HDI/PC), as shown in **Scheme S8**. A 10 wt% mixture of PEO (4 kDa, 1.06 Đ) in TCE flushed with N_2 gas was made. Once the diisocyanate

coupling reaction of BPA had run for 10 minutes, PEO dissolved in TCE was added in a 1:1 molar ratio of PEO hydroxyl groups to PC phenol groups, as shown in **Scheme S7**. Aliquots were taken at 0, 1, 2, 3, 4, and 5 hours. After the reaction ran for 19 hours, it was quenched with a 250 mL mixture of 1:10 IPA:hexane. Neither PC nor PEO is soluble in hexane, allowing for the polymer to precipitate. IPA was utilized to terminate the reaction by reacting with any residual isocyanate groups.

Scheme S7 End capping of Bisphenol-A (BPA) with 1,6-diisocyanatohexane (HDI) and then polymerization of Polyethylene oxide (PEO) oligomer with diisocyanate-BPA.

PC-PEO polymerization via diisocyanate coupling

A 50 mL round-bottom flask was charged with diphenol-capped PC (1g) and a stir bar, and then sealed with a septum. The round-bottom flask was flushed with N_2 gas, and then 10 mL of TCE was added. The vessel was placed in a 130 °C oil bath on a 250 RPM stir plate to allow the PC to dissolve in the THF. Once the PC was fully dissolved, HDI was added in a 2.05:1 molar ratio of isocyanate to phenol end groups (HDI/PC), as shown in **Scheme S8**. A 10 wt% mixture of PEO (4 kDa, 1.06 Đ) in TCE flushed with N_2 gas was made. Once the diisocyanate coupling reaction of PC had run for 10 minutes, PEO dissolved in TCE was added in a 1:1 molar ratio of PEO hydroxyl groups to PC phenol groups, as shown in **Scheme S8**. Aliquot was taken at 23 hours. After the reaction ran for 48 hours, it was quenched with a 250 mL mixture of 1:10 IPA:hexane. Neither PC nor PEO is soluble in hexane, allowing for the polymer to precipitate. IPA was utilized to terminate the reaction by reacting with any residual isocyanate groups.

Scheme S8 End capping of polycarbonate (PC) with 1,6-diisocyanatohexane (HDI) and then polymerization of Polyethylene oxide (PEO) oligomer with diisocyanate-PC.

Results

Polymerization of BHET-PEO MBCP

Figures S2-S6 demonstrate the formation and characterization of PEO-, BHET-, and BHET-PEO-based urethane polymers prepared via diisocyanate coupling. FTIR spectra in **Figure S2** track the evolution of PEO polymerized with HDI over time: the isocyanate stretching band (highlighted in the pink region) present at early times progressively disappears between 0 and 3 h, while urethane-associated bands (green region) grow in intensity, confirming consumption of NCO end groups and formation of urethane linkages between PEO chains. A similar behavior is observed for BHET-PEO coupling in **Figure S3**. Here, the 0 h BHET-PEO sample shows a distinct isocyanate band due to HDI activation of the BHET/PEO mixture, which is absent in the starting PEO and BHET precursors and subsequently diminishes as polymerization proceeds to 2 h, consistent with urethane formation between BHET and PEO segments.

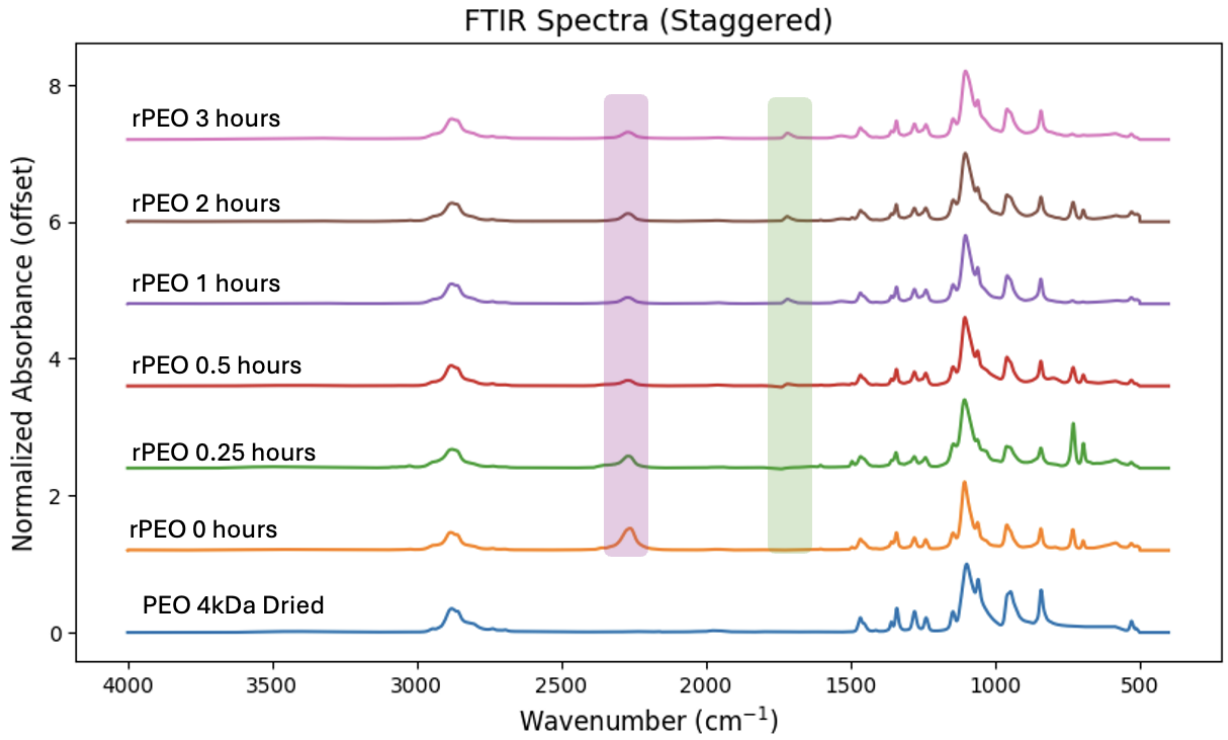

Figure S2 FTIR of PEO polymerized via diisocyanate coupling, with PEO (blue), 0 hour (orange), 0.25 hour (green), 0.5 hour (red), 1 hour (purple), 2 hours (brown), 3 hours (pink), highlighting the isocyanate group disappearing in the pink square and the urethane group forming with the green square.

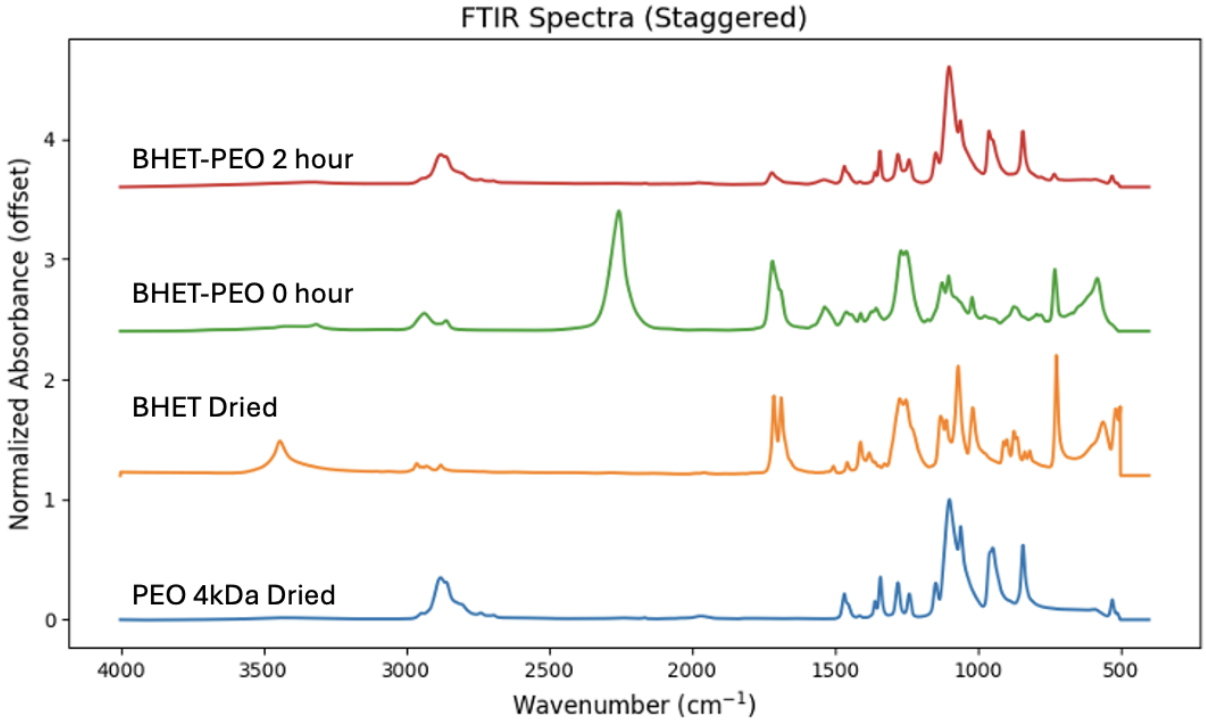

Figure S3 FTIR of BHET-PEO polymerized via diisocyanate coupling, with PEO (blue), BHET (orange), 0 hour (green), 2 hour (red). The isocyanate group is appearing in the 0 hour BHET-PEO sample.

^{1}H NMR and DOSY NMR provide complementary evidence for covalent connectivity in the BHET-PEO multiblocks. In **Figure S4**, the BHET spectrum displays characteristic methylene peaks β (4.4 ppm, green) and α (3.3 ppm, orange) to the hydroxyl group, along with aromatic resonances at 8.1 ppm (blue). PEO exhibits a single dominant methylene peak at 3.6 ppm (red). The BHET-PEO product combines all of these features, including BHET-derived methylene and aromatic peaks, the PEO methylene resonance, and additional methylene and urethane-associated signals from reacted HDI at 1.5-1.2 ppm (purple), confirming incorporation of all three components into a single polymer architecture. DOSY NMR of BHET-PEO (**Figure S5**) further supports this assignment: BHET- and PEO-derived resonances share a common diffusion coefficient in $CDCl_3$, indicating that both segments belong to the same diffusing macromolecule rather than existing as a simple physical mixture.

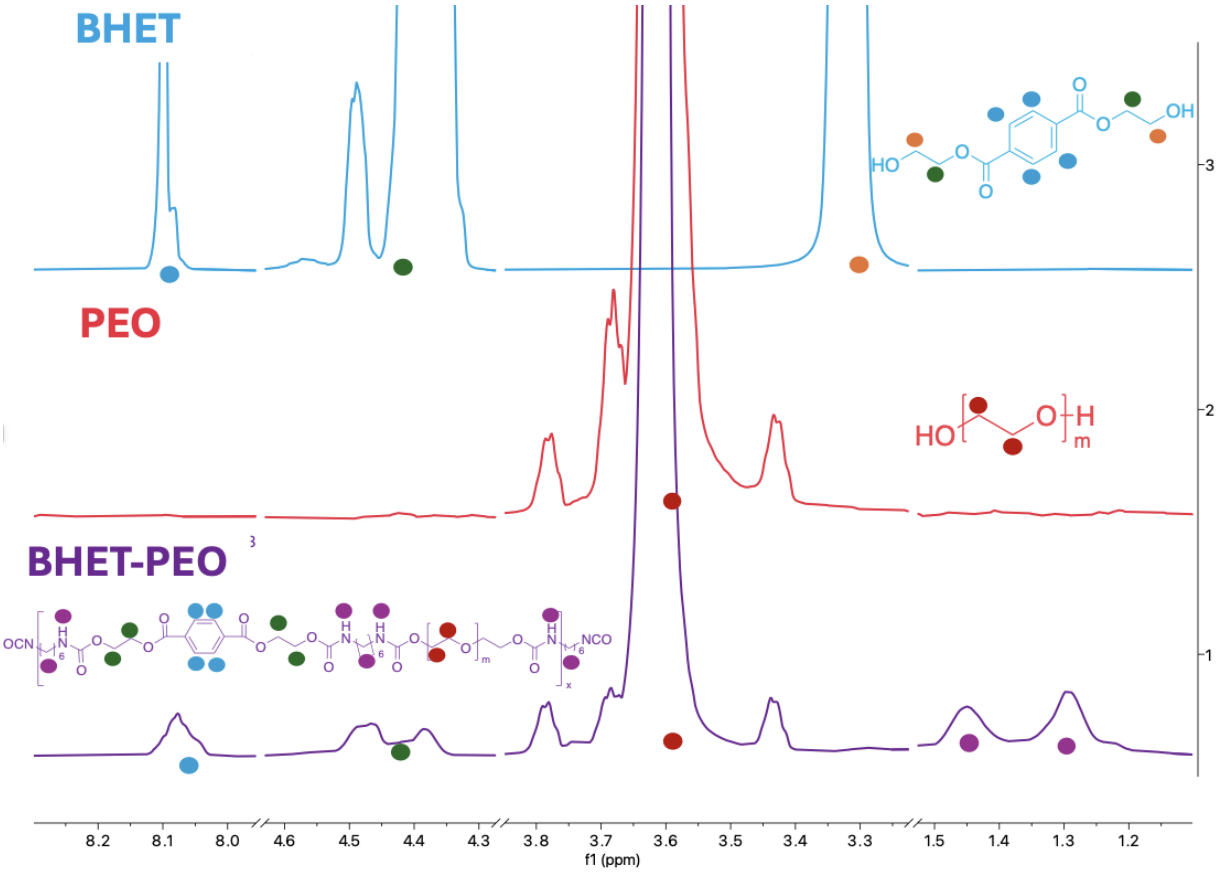

Figure S4 ^{1}H NMR of BHET (top, blue), PEO (middle, red), and BHET-PEO (bottom, purple) with their peaks of interest highlighted by the dots correlated to those peaks. BHET has methylene peaks in the beta position of the hydroxyl group (4.4 ppm, green) and the alpha position (3.3 ppm, orange), as well as aromatic peaks (8.1 ppm, blue). PEO shows a methylene peak at 3.6 ppm (red). BHET-PEO has methylene peaks from BHET (4.4 ppm, green) and PEO (3.6 ppm, red), aromatic peaks from BHET (8.1 ppm, blue), and methylene and urethane peaks from reacted HDI at 1.5-1.2 ppm (purple).

Figure S5 DOSY NMR of BHET-PEO in CDCl3 to demonstrate connectivity of PEO to BHET.

The impact of diisocyanate coupling on molar mass and dispersity is quantified in **Figure S6**. BHET homopolymers prepared with equimolar (1:1 OH:NCO) and excess isocyanate (1:2 OH:NCO) conditions (**Figure S6a**) show increased M_n and M_w upon coupling, with higher molar masses and modest changes in dispersity under NCO-rich conditions, consistent with more extensive chain extension and possible mild branching. Similarly, PEO homopolymers (**Figure S6b**) exhibit molar mass growth when reacted with HDI, with both 1:1 and 1:2 formulations yielding higher M_n and M_w relative to the starting oligomer while maintaining relatively narrow dispersity (Đ) values characteristic of step-growth urethane formation from telechelic chains. BHET-PEO multiblock copolymers synthesized under equimolar 1:1 OH:NCO conditions (**Figure S6c**) show clear increases in M_n and M_w relative to the individual BHET and PEO components, along with broadened but still controlled dispersities, indicating successful assembly of alternating

BHET and PEO segments into multiblock architectures. Collectively, **Figures S2-S6** establish that diisocyanate-mediated coupling provides a general strategy to convert BHET and PEO oligomers into well-defined urethane-linked homopolymers and multiblock copolymers with tunable molar masses and confirmed covalent connectivity.

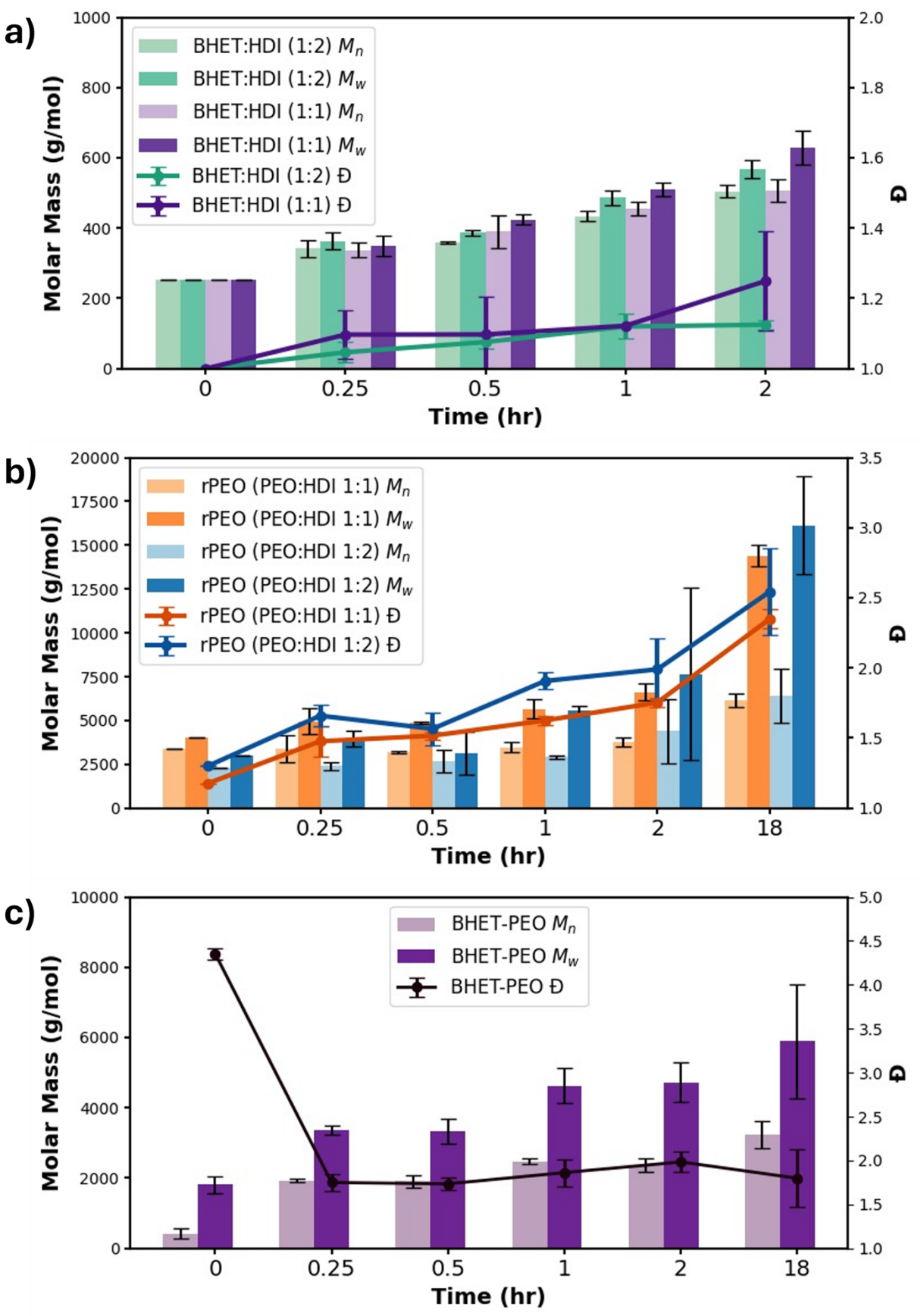
a)
BHET:HDI (1:2) M_n
BHET:HDI (1:2) M_w
BHET:HDI (1:1) M_n
BHET:HDI (1:1) M_w
BHET:HDI (1:2) Đ
BHET:HDI (1:1) Đ
Molar Mass (g/mol)
Đ
Time (hr)
b)
rPEO (PEO:HDI 1:1) M_n
rPEO (PEO:HDI 1:1) M_w
rPEO (PEO:HDI 1:2) M_n
rPEO (PEO:HDI 1:2) M_w
rPEO (PEO:HDI 1:1) Đ
rPEO (PEO:HDI 1:2) Đ
Molar Mass (g/mol)
Đ
Time (hr)
c)
BHET-PEO M_n
BHET-PEO M_w
BHET-PEO Đ
Molar Mass (g/mol)
Đ
Time (hr)

Figure S6(a-c) Change in molar mass and dispersity of BHET, PEO, and BHET-PEO polymerization via diisocyanate coupling. **(a)** BHET was polymerized with equimolar (1:1, light purple bar-M_n, purple bar-M_w, dark purple line-dispersity (*Đ*),) and excess isocyanate (1:2, light green bar-M_n, green bar-M_w, dark green line-*Đ*) relative to hydroxyl end groups (OH:NCO). **(b)** PEO was polymerized with equimolar (1:1, light orange bar-M_n, orange bar-M_w, dark orange line-*Đ*) and excess isocyanate (1:2, light blue bar-M_n, blue bar-M_w, dark blue line-*Đ*) relative to hydroxyl end groups. **(c)** BHET-PEO multiblock copolymers were polymerized with equimolar (1:1, light purple bar-M_n, purple bar-M_w, black line-*Đ*) relative to hydroxyl end groups.

PET Repolymerization

Table S1 and **Figures S7** and **1(f)** characterize the depolymerized PET (dPET) obtained in trial 1 and its subsequent repolymerization with hexamethylene diisocyanate (HDI). Relative to virgin PET, which exhibits high molar mass (M_n = 20.8 kDa, M_w = 54.9 kDa, Đ = 2.64) and an average of ~1 hydroxyl end group per chain, dPET trial 1 displays a modestly reduced molar mass (M_n = 16.8 kDa, M_w = 29.2 kDa) and increased hydroxyl functionality (1.71 -OH end groups per chain), consistent with controlled chain scission that generates telechelic oligomers rather than severely degraded fragments. The higher viscosity-average molar mass (M_v = 28.2 kDa) further confirms that dPET retains a substantial chain length suitable for rechain extension. As shown in our previous work,[4] the yield of PET oligomers remains high when the oligomers are not dihydroxy-capped.

Table S1: Molar mass, dispersity, average number of hydroxyl groups per chain, and isolated yield for virgin PET and depolymerized PET (dPET) trial 1.

Sample	M_n (kg/mol)	M_v (kg/mol)	M_w (kg/mol)	*Đ*	-OH end groups	Yield
dPET Trial 1	16.8	28.2	29.2	1.7	1.71	101.7%
Virgin PET	20.8	54.1	54.9	2.6	1.00	

^{1}H NMR spectra in **Figure S7** track the reaction of dPET with HDI at different OH:NCO molar ratios. The dPET spectrum shows characteristic aromatic and aliphatic PET backbone resonances (blue and green circles) along with methylene protons α to hydroxyl end groups (purple circle), reflecting the increased population of -OH-terminated chains. Upon reaction with HDI at

1:2 OH:NCO and 1:1 OH:NCO, new signals corresponding to HDI-derived aliphatic protons (orange circle) appear while hydroxyl end-group resonances diminish, indicating the formation of urethane linkages and effective consumption of reactive chain ends. **Figure 1(f)** quantifies the impact of stoichiometry and reaction time on chain growth: the viscosity-average molar mass (M_v) of dPET trial 1 increases for both 1:1 and 1:2 PET:HDI formulations between 0 and 24 h, with higher Mv values observed under the more isocyanate-rich 1:2 conditions, consistent with more extensive chain extension and/or mild branching. Together, **Table S1** and **Figures S7** and **1(f)** demonstrate that dPET trial 1 serves as a reactive, hydroxyl-terminated oligomer feedstock that can be efficiently repolymerized via diisocyanate coupling to recover or exceed the molar masses of the starting PET resin.

Figure S7 ^{1}H NMR of depolymerized PET (dPET, top blue), PET polymerized with 1:2 OH:NCO molar ratio (PET:HDI (1:2), green middle), PET polymerized with 1:1 OH:NCO molar ratio (PET:HDI (1:1), red bottom) in a mixture of HFIP:$CDCl_3$. The polymerization scheme at the top

is highlighted with a colored circle that correlates to peaks in the spectrum, also shown at the bottom of the spectrum. The purple circle correlates to the methylene protons in the alpha position to the hydroxyl end group; the blue circle correlates to the aromatic protons in the PET backbone; the green circle correlates to the aliphatic protons in the PET backbone; the orange circle correlates to the aliphatic protons from HDI; the black circle correlates to the methylene protons from the isopropanol end group. Reactions were quenched with isopropanol to consume remaining -NCO groups; these rPET samples are not used in subsequent PET-PEO multiblock synthesis.

Depolymerization of PET

Figures S8-S9 and **Table S2** characterize the molar mass, end-group structure, and chain architecture of virgin PET and depolymerized PET (dPET) oligomers. Normalized GPC traces in **Figure S8** show that both dPET trial 2 and trial 3 are shifted substantially to lower molar mass relative to virgin PET, consistent with controlled chain scission during glycolysis. The dPET samples retain relatively narrow dispersities ($Đ \approx 1.5$-1.9) compared to the parent polymer ($Đ \approx 1.97$), indicating the formation of telechelic oligomers rather than broad, highly degraded distributions. Quantitative GPC analysis (**Table S2**) confirms that M_n decreases from ~16 kDa for virgin PET to ~5.6-5.8 kDa for dPET trials 2 and 3, while the average number of hydroxyl end groups per chain increases from ~1.1 in virgin PET to ~2.0 in the dPET samples, demonstrating efficient generation of dihydroxyl-terminated PET oligomers suitable for subsequent coupling reactions.

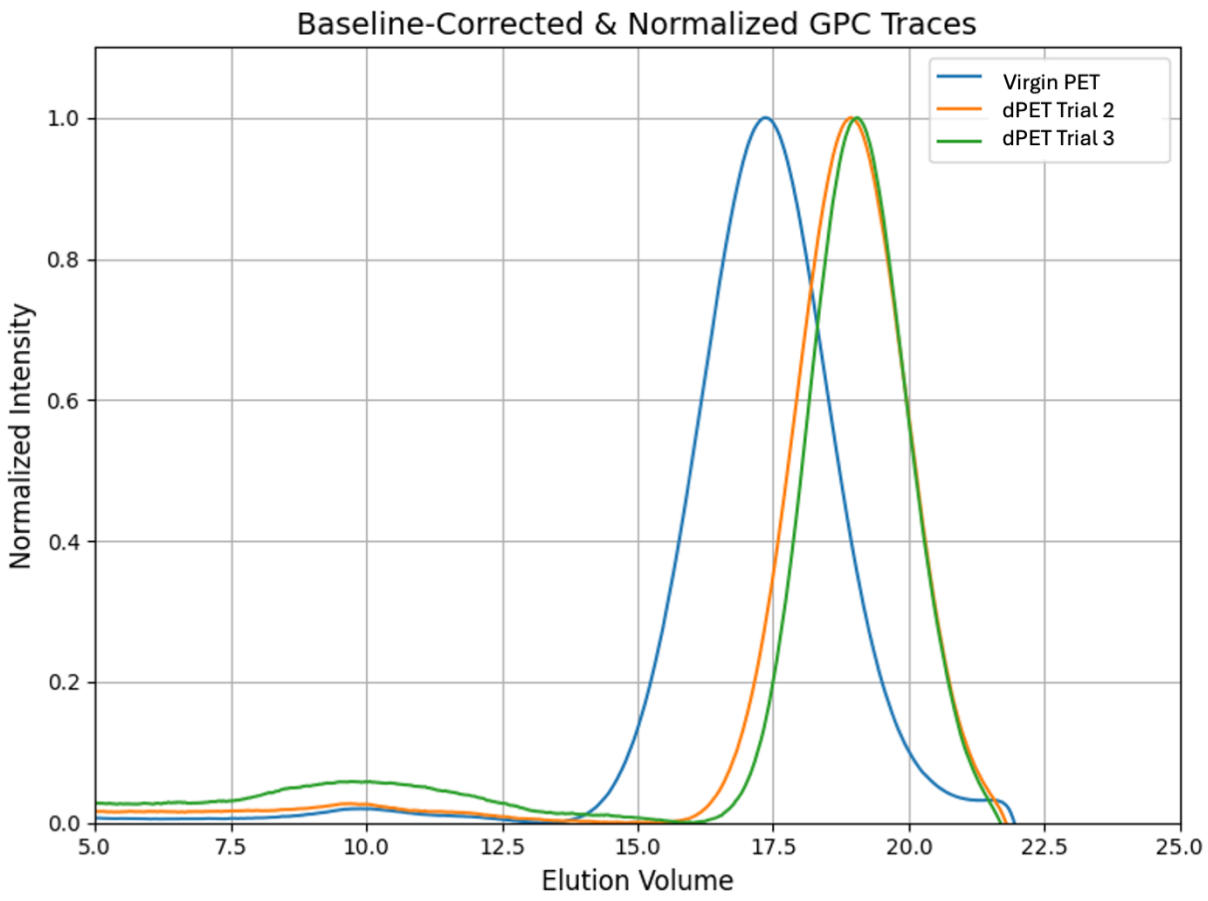

Figure S8 Normalized GPC trace of virgin PET (blue), depolymerized PET (dPET) trial 2 (orange), and dPET trial 3 (green).

Structural assignments from ^{1}H NMR (**Figure S9**) further verify the identity and end-group functionality of the dPET oligomers. In spectra collected in HFIP:$CDCl_3$, the aromatic and aliphatic backbone resonances of PET (blue and green circles, respectively) are preserved in both dPET trials, confirming that the repeat-unit structure of the polyester is maintained after depolymerization. In addition, a distinct resonance corresponding to methylene protons α to hydroxyl end groups (purple circle) is clearly observed in the dPET spectra but is much less prominent in virgin PET, consistent with an increased population of hydroxyl-terminated chain ends. Together, the GPC and NMR data in **Figures S8-S9** and **Table S2** show that glycolysis converts high-molecular-weight PET into well-defined, dihydroxyl-terminated oligomers with controlled chain lengths and sufficient functionality for subsequent multiblock copolymer

synthesis. Depolymerization affords dihydroxy-terminated PET oligomers in moderate to high yields suitable for subsequent multiblock copolymerization.

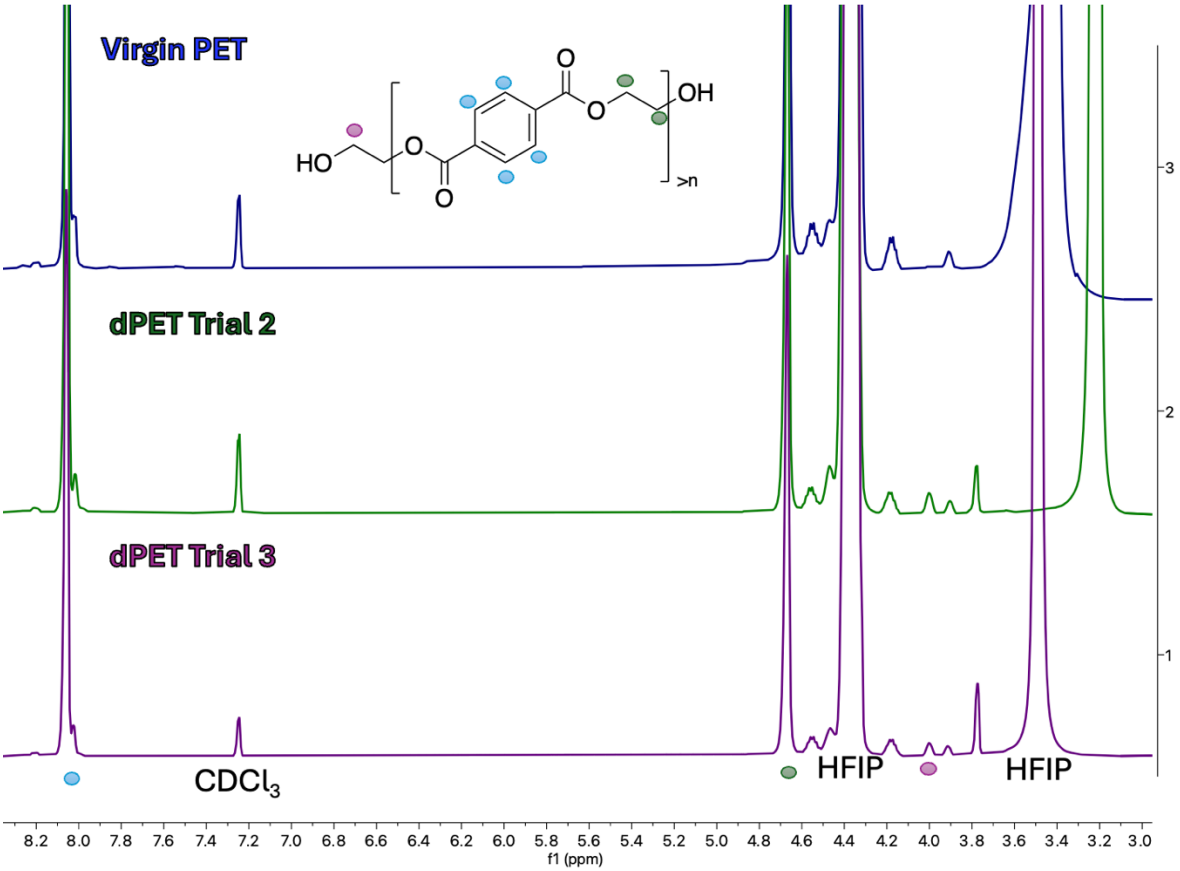

Figure S9 ^{1}H NMR of virgin PET (top blue), depolymerized PET (dPET) trial 2 (green middle), and dPET trial 3 (purple bottom) in a mixture of HFIP:$CDCl_3$. The PET scheme at the top is highlighted with a colored circle that corresponds to peaks in the spectrum, which are also shown at the bottom of the spectrum. The purple circle correlates to the methylene protons in the alpha position to the hydroxyl end group; the blue circle correlates to the aromatic protons in the PET backbone; the green circle correlates to the aliphatic protons in the PET backbone.

Table S2 Molar mass, dispersity, average number of hydroxyl groups per chain, and isolated yield for virgin PET and depolymerized PET (dPET) trials 2 and 3.

Sample	M_n (kg/mol)	M_w (kg/mol)	$Đ$	-OH end groups	Yield
dPET Trial 3	5.8	8.9	1.5	1.97	54%
dPET Trial 2	5.6	10.5	1.9	2.0	79%
Virgin PET	16.0	31.6	2.0	1.13	

PET-PEO Polymerization

Figures S10-S11 collectively demonstrate the time-dependent growth and covalent connectivity of PET-PEO multiblock copolymers prepared via short HDI end-capping. Complementary to **Figure 2(b)**, ^{1}H NMR data in **Figure S10** provide molecular-level evidence for urethane bond formation: the spectra reveal **(a)** the emergence of new resonances corresponding to urethane linkages, **(b)** increasing urethane signal intensity with reaction time, indicating rapid consumption of residual isocyanate end groups, and **(c)** the disappearance of hydroxyl end-group resonances, confirming that the reactive chain ends are being converted into covalent PET-PEO junctions. DOSY NMR spectra in **Figure S11** further validate this connectivity; for samples reacted 4, 9, and 22 h, PET- and PEO-derived resonances share common diffusion coefficients in HFIP:$CDCl_3$, demonstrating that the aromatic polyester and polyether segments reside within a single diffusing species rather than existing as separate homopolymers or simple blends. Together, these results confirm efficient formation of PET-PEO multiblock architectures under short HDI end-capping conditions, with molar mass and extent of coupling increasing systematically with reaction time.

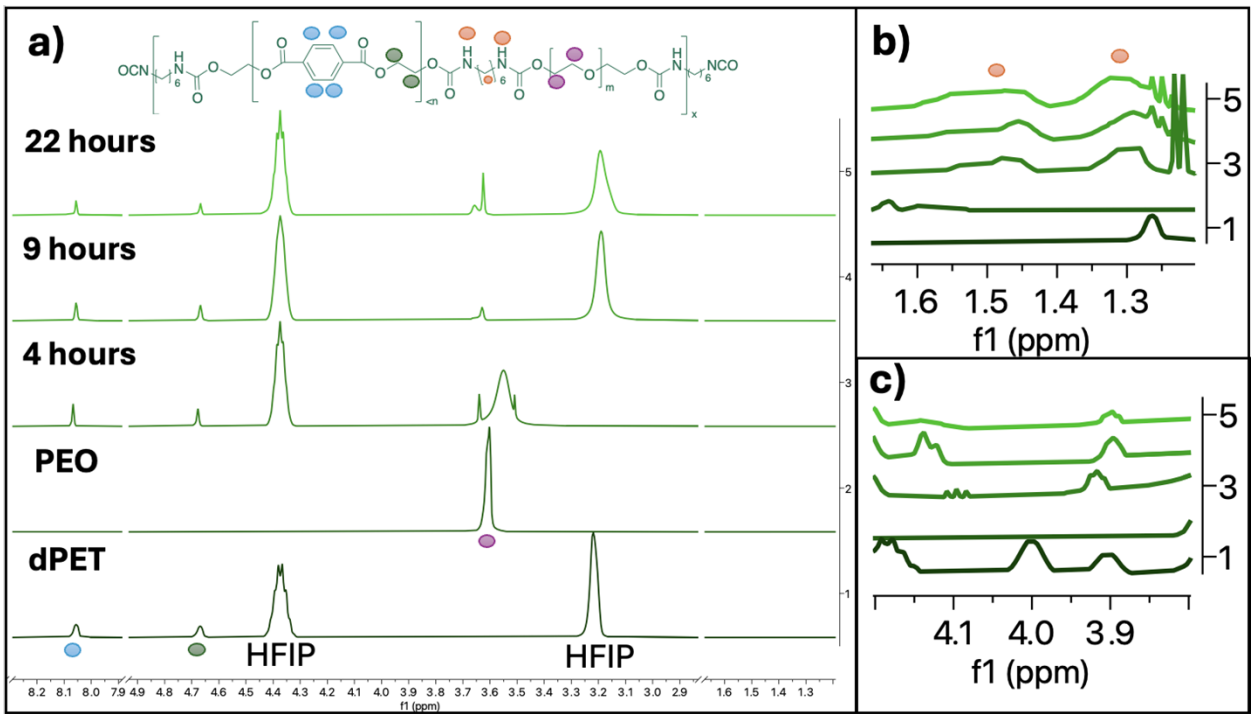

Figure S10 (a) ^{1}H NMR spectra of PET-PEO samples after PEO addition, **(b)** increasing urethane-group intensity with reaction time, indicating the rapid consumption of residual isocyanate end groups and **(c)** showing the disappearance of hydroxyl end-group resonances.

Figure S11 DOSY NMR of short end-capped PET-PEO reacted for 4, 9, and 22 hours, in a mixture of HFIP:$CDCl_3$ to demonstrate connectivity of PEO to PET.

The relative PET content in the PET-PEO multiblock copolymers was quantified by ^{1}H NMR, integrating aliphatic proton resonances specific to each segment and relating them to the underlying repeat-unit structures. For a given oligomer, the degree of polymerization *n* was estimated from the number-average molar mass (M_n) obtained by NMR using **Equation S1**, where M_o is the monomer repeat-unit molar mass. The total number of aliphatic protons in the polymer

chain ($H_{polymer}$) was then calculated from the number of aliphatic protons per repeat unit ($H_{monomer}$) via **Equation S2**. For multiblock PET-PEO copolymers, the PET proton fraction f_{PET} was defined as the ratio of PET-derived aliphatic protons (H_{PET}) to the total aliphatic protons from both PET and PEO ($H_{PET} + H_{PEO}$), as given in **Equation S3**.

$$n = \frac{M_n}{M_o} \quad \textbf{(S1)}$$

$$Aliphatic\ Protons = H_{polymer} = n * H_{monomer} \quad \textbf{(S2)}$$

$$f_{PET} = \frac{H_{PET}}{H_{PET} + H_{PEO}} \quad \textbf{(S3)}$$

$$PET/PEO\ Ratio = \frac{f_{PET\ -\ observed}}{f_{PET\ -\ expected\ (1:1)}} \quad \textbf{(S4)}$$

For a system prepared from dPET trial 2 and PEO oligomers mixed in a 1:1 molar ratio, the expected PET proton fraction is 0.24 based on the known repeat-unit compositions. To compare different samples to this idealized case, the observed PET fractions ($f_{PET\text{-}observed}$) were normalized to the theoretical 1:1 value ($f_{PET\text{-}expected(1:1)}$) using **Equation S4**. The PET/PEO ratio is defined as the molar ratio of PET repeat units to PEO repeat units in the multiblock copolymer, determined from ^{1}H NMR peak integrals. **Table S3** summarizes the expected 1:1 f_{PET} and the observed f_{PET} values for short and long HDI end-capped PET-PEO samples, along with their corresponding PET/PEO ratios. The dPET trial 2 and trial 3 1:1 mixtures give $f_{PET} \approx 0.24$-0.25 and PET/PEO ratios of 1.00, as expected for ideal stoichiometry. In contrast, the short end-capped PET-PEO samples at 4 and 9 h exhibit higher PET fractions ($f_{PET} \approx 0.37$-0.39, PET/PEO ratios ≈ 1.55-1.60), indicating PET-enriched compositions relative to the nominal 1:1 ratio, while the 22 h short end-capped sample ($f_{PET} = 0.22$, PET/PEO ratios = 0.93) is slightly PET-deficient. The long end-capped PET-PEO sample at 22 h shows the highest PET enrichment ($f_{PET} = 0.42$, PET/PEO ratios = 1.67), consistent with preferential PET incorporation and/or more efficient coupling of PET-derived oligomers under extended end-capping conditions.

Table S3 Theoretical PET proton fraction expected for ideal 1:1 PET-PEO oligomer incorporation, observed PET proton fractions determined by ^{1}H NMR for short and long HDI end-capped PET-PEO samples, and corresponding PET/PEO ratios values.

Sample	f_{PET}	PET/PEO ratios
(1:1) dPET trial 2:PEO	0.24	1.00
(1:1) dPET trial 3:PEO	0.25	1.00
***Short end-caping* PET-PEO 4 hours**	0.39	1.60
***Short end-caping* PET-PEO 9 hours**	0.37	1.55
***Short end-caping* PET-PEO 22 hours**	0.22	0.93
***Long end-caping* PET-PEO 22 hours**	0.42	1.67

Figures S12 and **S13** provide additional evidence for the successful formation of PET-PEO multiblock copolymers via HDI-mediated coupling and highlight the impact of end-capping time on molecular architecture. GPC traces in **Figure S12** compare samples prepared using short (10 min) and extended (24 h) HDI end-capping prior to PEO addition. DOSY NMR analysis of the 24 h PET-PEO multiblock copolymer (**Figure S13**) further confirms covalent incorporation of both components into a single macromolecular species. The PET and PEO resonances share a common diffusion coefficient, distinct from those of the corresponding homopolymers, demonstrating that the aromatic polyester and polyether segments diffuse together rather than as separate entities. Together, **Figures S12** and **S13** show that extended HDI end-capping still forms multiblock copolymers by increasing molar mass, while diffusion-ordered NMR spectroscopy verifies that PET and PEO segments are covalently linked within the same diffusing chains rather than forming simple physical blends or mixtures.

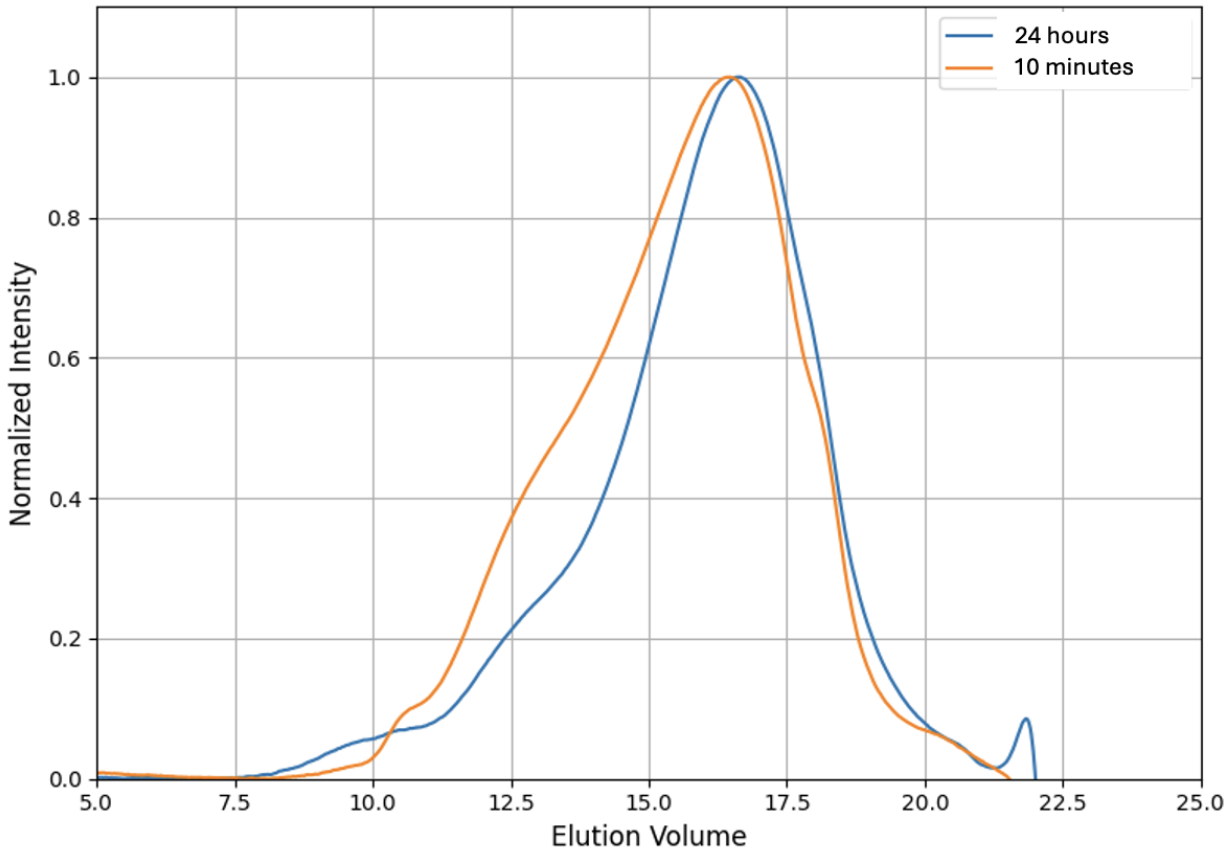

Figure S12 GPC traces of PET-PEO multiblock copolymers prepared using short (10 min, orange) and extended (24 h, blue) HDI end-capping prior to PEO addition, illustrating differences in molar mass distribution and dispersity.

Figure S13 DOSY NMR spectrum of the PET-PEO multiblock copolymer prepared using extended HDI end-capping (24 h), showing coincident diffusion coefficients for PET and PEO resonances, consistent with covalent incorporation of both segments into a single diffusing species.

Mechanical Testing

Figures S14-S18 highlight the mechanical response and film-forming behavior of virgin PET, PET-PEO multiblock copolymers, and related solvent-cast blends. Stress-strain curves for solvent-cast virgin PET (**Figure S14**) exhibit the expected stiff, relatively brittle response characteristic of a glassy polyester, with high modulus and limited elongation at break. In contrast, the 24 h end-capped PET-PEO multiblock copolymer (**Figure S15**) shows reduced stiffness and enhanced ductility relative to virgin PET, consistent with incorporation of soft PEO segments into a continuous PET-rich network. The 10 min end-capped PET-PEO sample (**Figure S16**), which contains shorter multiblock chains and a higher fraction of low-molecular-weight species, displays an intermediate mechanical response, reflecting partial softening and toughening but less extensive

network formation than in the fully reacted 24 h material. The compatibilized PET/PEO 80:20 blend (**Figure S17**) has lower strength then virgin PET and lower elongation than the PET-PEO MBCPs.

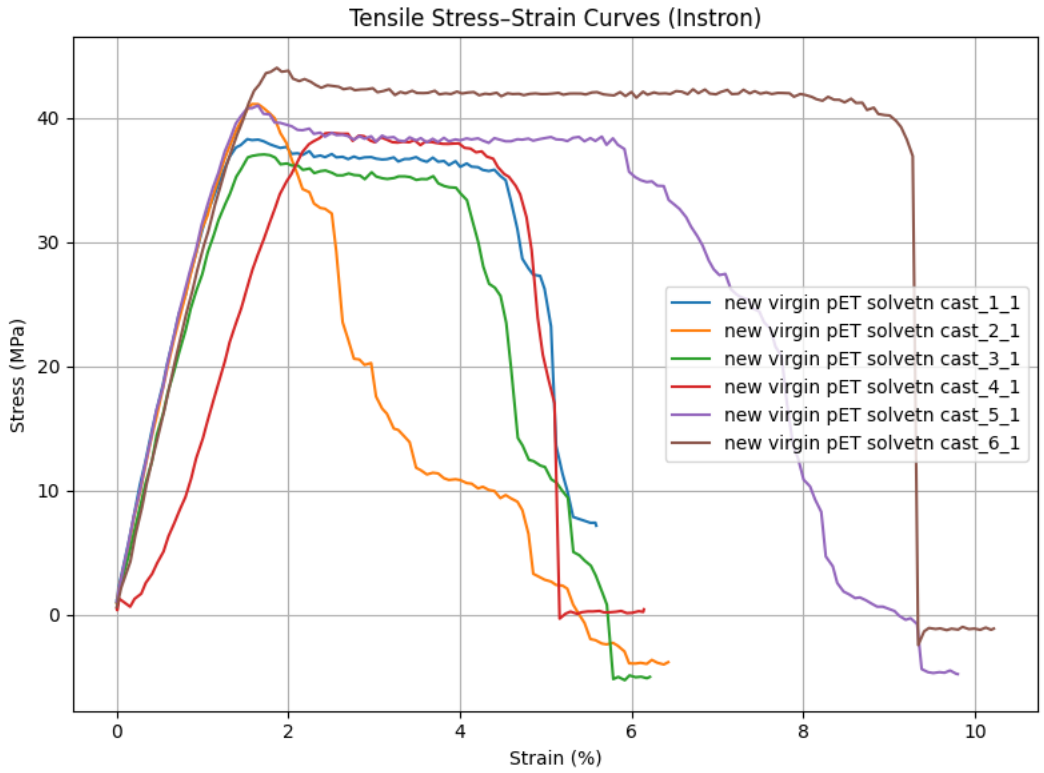

Figure S14 Stress vs Strain curves of virgin PET that was solvent cast

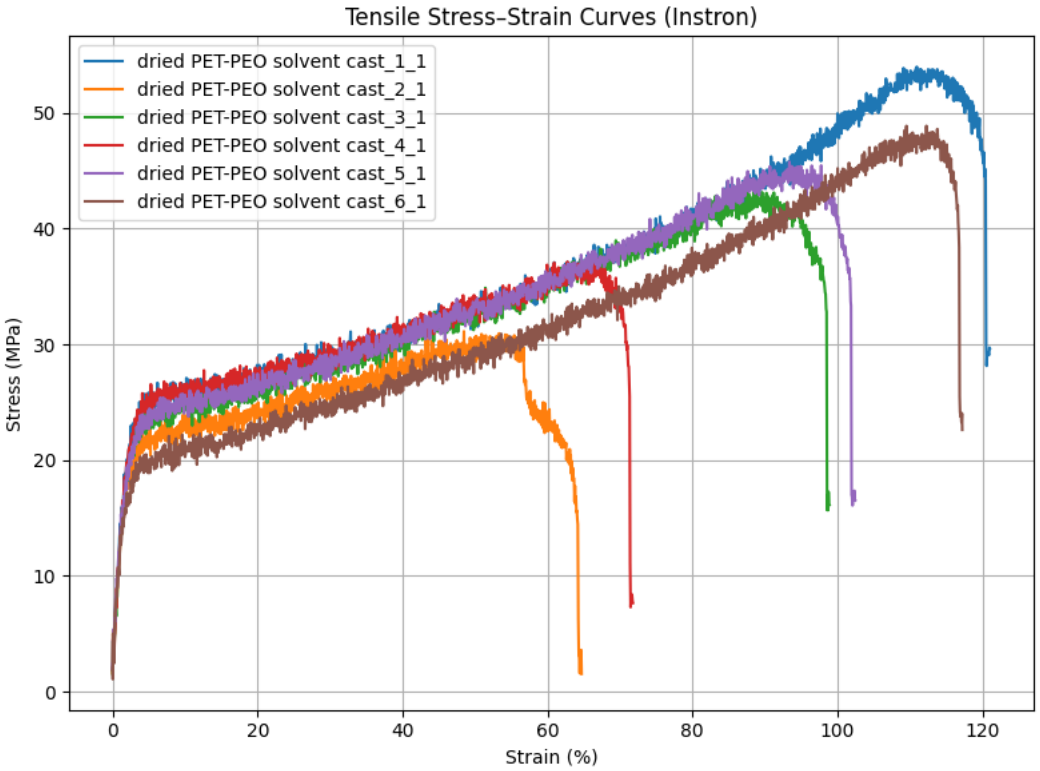

Figure S15 Stress vs Strain curves of PET-PEO (24-hour end-capped) that was solvent cast

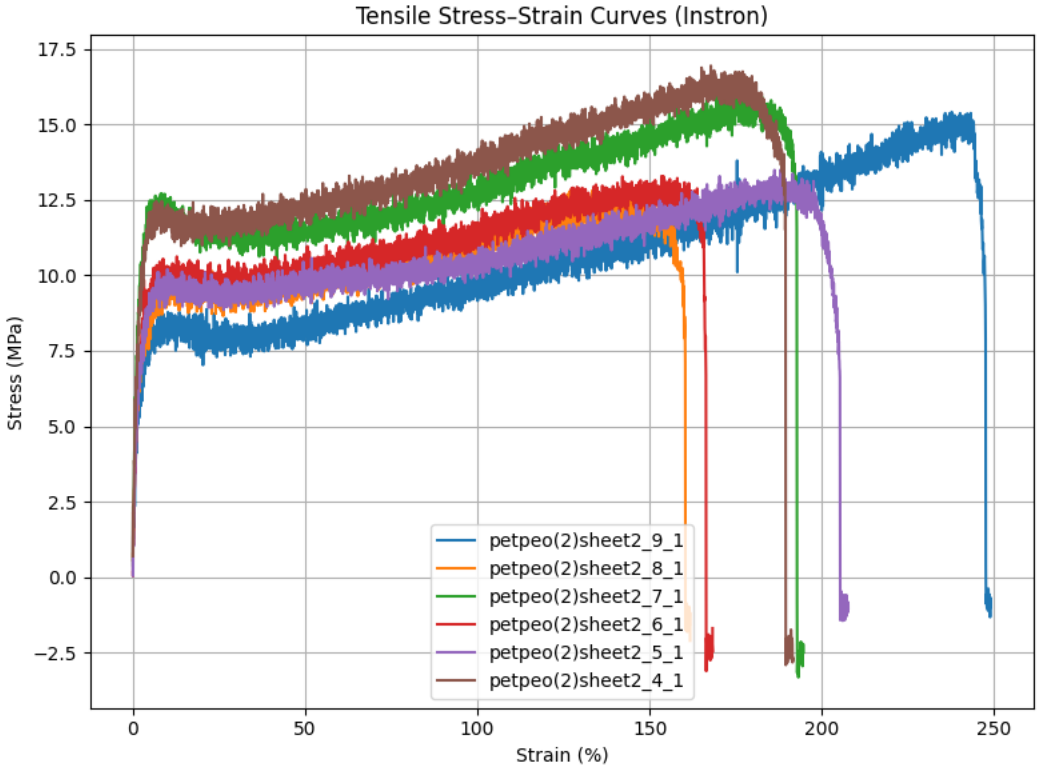

Figure S16 Stress vs Strain curves of PET-PEO (10 min end-capped) that was solvent cast

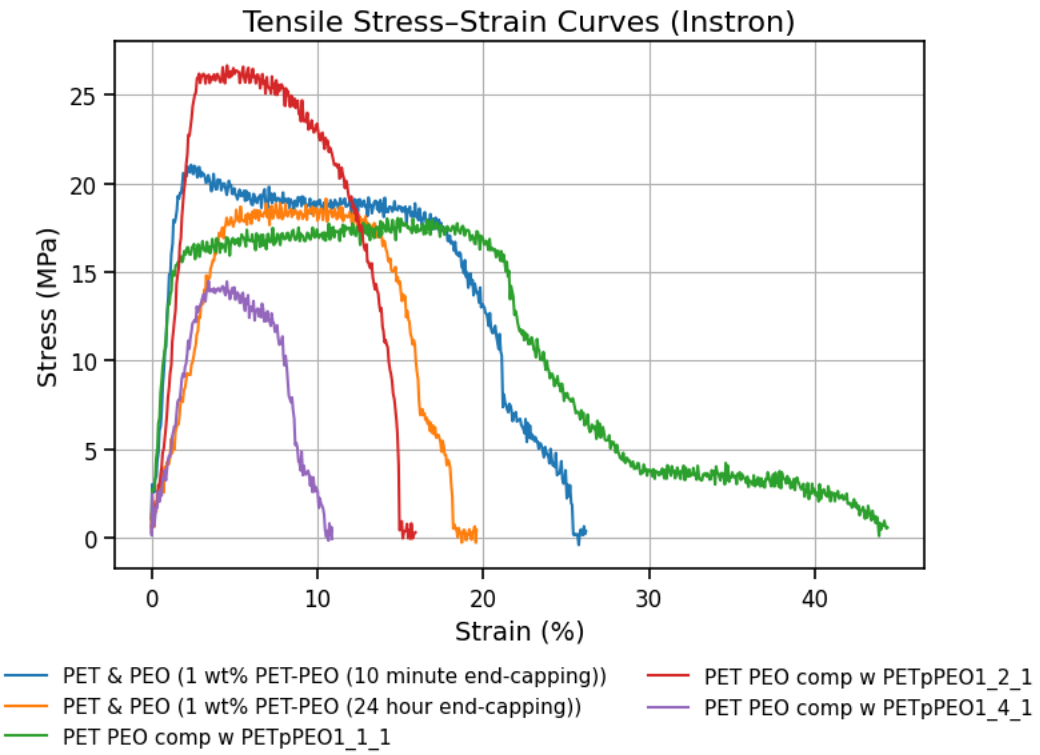

Figure S17 Stress vs Strain curves of 80:20 PET/PEO blend compatibilized with 1 wt% PET-PEO multiblock copolymer

Photographs of failed solvent-cast films (**Figure S18**) further emphasize the role of compatibilization and molecular architecture in determining processability. A 50:50 blend of PET and PEO homopolymers exhibits poor film integrity, indicating limited interfacial adhesion between the immiscible phases. Adding 1 wt% of the short end-capped PET-PEO MBCP improves film continuity in the 50:50 PET:PEO blend, consistent with its role as a compatibilizer that bridges the PET and PEO phases. In contrast, the repolymerized PEO ($M_n \approx 38.3$ kDa) alone forms films with markedly different failure characteristics, reflecting its low glass transition temperature and absence of a reinforcing PET phase. Together, **Figures S14-S18** demonstrate that introducing PET-PEO multiblock architectures, either as the primary matrix or as a minor compatibilizing component, substantially modifies mechanical performance and film quality relative to simple PET/PEO homopolymer blends.

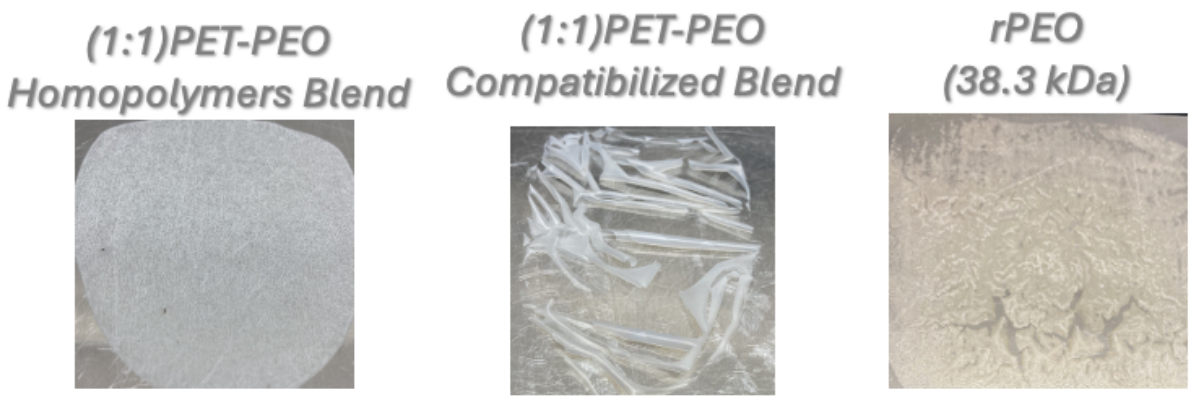

Figure S18 Images of failed solvent cast films. From left to right: 50/50 blend of PET:PEO homopolymers, 50/50 blend of PET:PEO homopolymers that were compatibilized with 1 wt% of the short end-capped PET-PEO MBCP, repolymerized PEO (38.3 kDa).

Table S4 shows the DCS was used to probe how block architecture and end-capping conditions influence the crystallization behavior of PET and PEO in the PET-PEO systems. Virgin PET exhibits a relatively high heat of fusion (ΔH_f, PET = 37.8 J/g), which decreases in rPET (25.75 J/g), consistent with a reduction in crystallinity due to the introduction of aliphatic chains. In the 80:20 PET:PEO physical blend, distinct melting endotherms corresponding to both polymers are observed (ΔH_f, PET = 18.53 J/g and ΔH_f, PEO = 23.4 J/g), indicating that PET and PEO can crystallize largely independently when not covalently tethered. In contrast, the end-capped PET-PEO block copolymers show a strong dependence of PEO crystallinity on block length and end-capping time. For the short end-capped series (10 minutes), the 4-hour sample displays a high PET heat of fusion (46.4 J/g) but no detectable PEO melting, suggesting that PET crystallization dominates and constrains the relatively short PEO blocks, suppressing their ability to form stable lamellae. With increasing polymerization time to 9 hours and 22 hours, PET crystallinity progressively decreases (ΔH_f, PET = 39.67 and 25.4 J/g, respectively), while the PEO heat of fusion increases from 1.54 to 10.01 J/g, implying that changes in block architecture and/or composition gradually relieve some of the confinement and enable PEO crystallization. By contrast, the long end-capped PET-PEO sample at 22 hours maintains a measurable PET heat of

fusion (19.99 J/g) but again shows no detectable PEO melting. This outcome is consistent with a morphology in which extended PET blocks form dominant crystalline domains, while the tethered, shorter PEO blocks are confined to interlamellar or interfacial regions and cannot organize into sufficiently large or well-ordered crystallites to produce a distinct PEO melting endotherm.

Table S4. Heats of fusion (ΔH_f) for PET and PEO segments in virgin PET, rPET, an 80:20 PET/PEO physical blend, and PET-PEO copolymers subjected to different end-capping conditions, as determined by DSC.

Sample	**PET** ΔH_f	**PEO** ΔH_f
Virgin PET	37.8	N/A
rPET	25.75	N/A
80:20 PET:PEO blend	18.53	23.4
Short end-capped **PET-PEO 4 hours**	46.4	0
Short end-capped **PET-PEO 9 hours**	39.67	1.54
Short end-capped **PET-PEO 22 hours**	25.4	10.01
Long end-capped **PET-PEO 22 hours**	19.99	0

Small- and Wide-Angle X-ray Scattering (SAXS/WAXS)

SAXS and WAXS measurements were carried out on solvent-cast films of repolymerized PET (rPET), PET-PEO multiblock copolymers (10 min end-capped at various reaction times and 24 h end-capped), and 80:20 PET/PEO blends. The WAXS patterns (**Figure S19**) show the characteristic PET crystalline reflections in all PET-containing samples, with reduced intensity and slight peak broadening in rPET and multiblock samples, consistent with the lower crystallinity inferred from DSC (**Table S4**). Additional broad scattering features appear in the multiblock and blend samples, but no distinct peaks can be confidently assigned to PEO crystallites based on literature reference patterns.

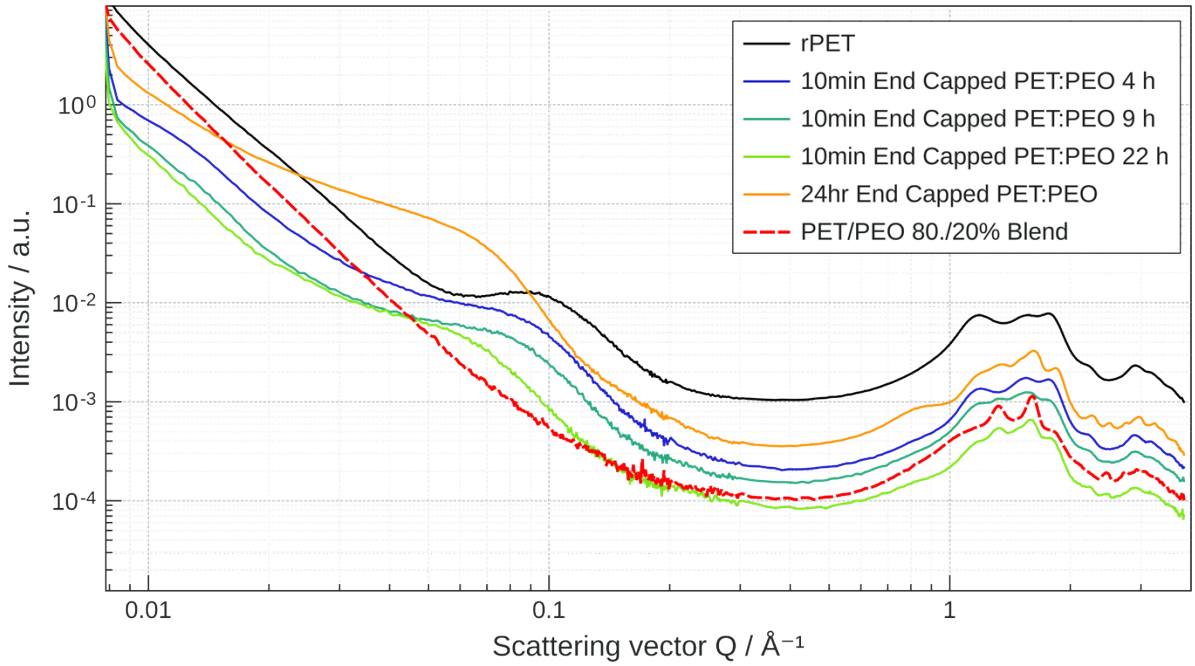

Figure S19. SAXS and WAXS patterns of rPET (black), PET-PEO multiblock copolymers (10 min end-capped (4h blue, 9 hour green, 22 hour light green) and 24 h end-capped (orange)), and an 80:20 PET/PEO blend (dashed red line). WAXS shows PET crystalline reflections in all PET-containing samples and additional broad features in the multiblock and blend films. SAXS profiles of the same films display broad maxima characteristic of semicrystalline lamellar morphology but no well-resolved higher-order peaks indicative of long-range ordered microphase separation.

SAXS profiles (**Figure S19**) exhibit broad scattering maxima consistent with semicrystalline lamellar morphology in PET-containing samples. However, there are no well-developed higher-order peak series observed that would indicate the formation of microphase separated domains that may be expected of block-copolymers. The PET-PEO multi-blocks show subtle changes in the position and intensity of the primary SAXS maximum relative to virgin PET and rPET, suggesting changes in lamellar thickness and/or long-period spacing, but the data do not support the identification of well-ordered microphase-separated domains. SAXS/WAXS therefore primarily corroborates the presence and relative amount of PET and PEO crystalline

phases, while relying on DSC as the main tool for quantifying crystallinity and identifying which blocks crystallize in each material.

Gas permeation

Table S5 summarizes gas permeabilities of He, H_2, N_2, CH_4, CO_2, and O_2 for literature PolyActive materials, PET of varying densities, and the short-end-capped PET-PEO MBCP and compatibilized PET:PEO blend examined in this work. Compared with dense PET, which exhibits low N_2 and O_2 permeabilities characteristic of a tightly packed, glassy polyester, PolyActive samples show substantially higher gas permeabilities, consistent with their higher PEO content and more rubbery character. The short-end-capped PET-PEO MBCP displays permeabilities that are one to two orders of magnitude greater than PET for all measured gases, with particularly high values for He, H_2, and CO_2, reflecting transport dominated by hydrated PEO-rich domains rather than diffusion through the PET matrix. In contrast, the 80:20 compatibilized PET:PEO blend shows only modest increases in permeability relative to PET, maintaining gas transport characteristics closer to the virgin PET phase while still benefiting from limited PEO-mediated transport.

Table S5: Literature values for PolyActive[5,6] and PET, and experimental values for short-end-capped PET-PEO MBCP and an 80:20 compatibilized (1 wt%) blend of PET:PEO homopolymers permeated with He, H_2, N_2, CH_4, CO_2, and O_2.

Sample	He	H_2	N_2	CH_4	CO_2	O_2
PolyActive ($4000PEO_{55}PBT_{45}$)[6]	---	10.55	2.61	6.76	112	---
PolyActive (PEO-PBT/GO-0)[5]	---	14.3	2.88	8.4	150	---
PET (Density 0.967)	---	---	0.15	---	---	0.47
PET (Density 0.964)	---	---	0.185	---	---	0.57
PET (Density 0.954)	2.5	---	0.29	---	1.6	0.9
PET (Density 0.943)	3.8	---	0.48	---	2	1.5
PET-PEO (10-min End-Capped)	138.59	243.69	52.31	22.51	223.95	197.36
PET:PEO Blend (80:20)-Compatibilized	6.86	5.22	16.18	15.33	19.52	17.74

Figure S20 presents Robeson plots of gas permeability-selectivity performance for CO_2/N_2, O_2/N_2, H_2/N_2, He/N_2, and H_2/CH_4 pairs, comparing the short-end-capped PET-PEO MBCP and compatibilized PET:PEO blend with literature data for PolyActive and PET. Across all gas pairs, PET data cluster at low permeability with comparatively high selectivity, whereas PolyActive and the PET-PEO MBCP occupy a high-permeability regime with reduced selectivity, often approaching but not surpassing the 1991, 2008, and 2015 Robeson upper bounds. The compatibilized PET:PEO blend lies between these extremes, exhibiting moderate permeability enhancements over PET with only a partial loss in selectivity. Taken together, **Table S5** and **Figure S20** demonstrate that extensive PEO incorporation via multiblock copolymerization drives a transition to PEO-dominated gas transport, while compatibilized blends offer a more conservative route to tuning permeability-selectivity trade-offs without catastrophic loss of transport discrimination relative to virgin PET.

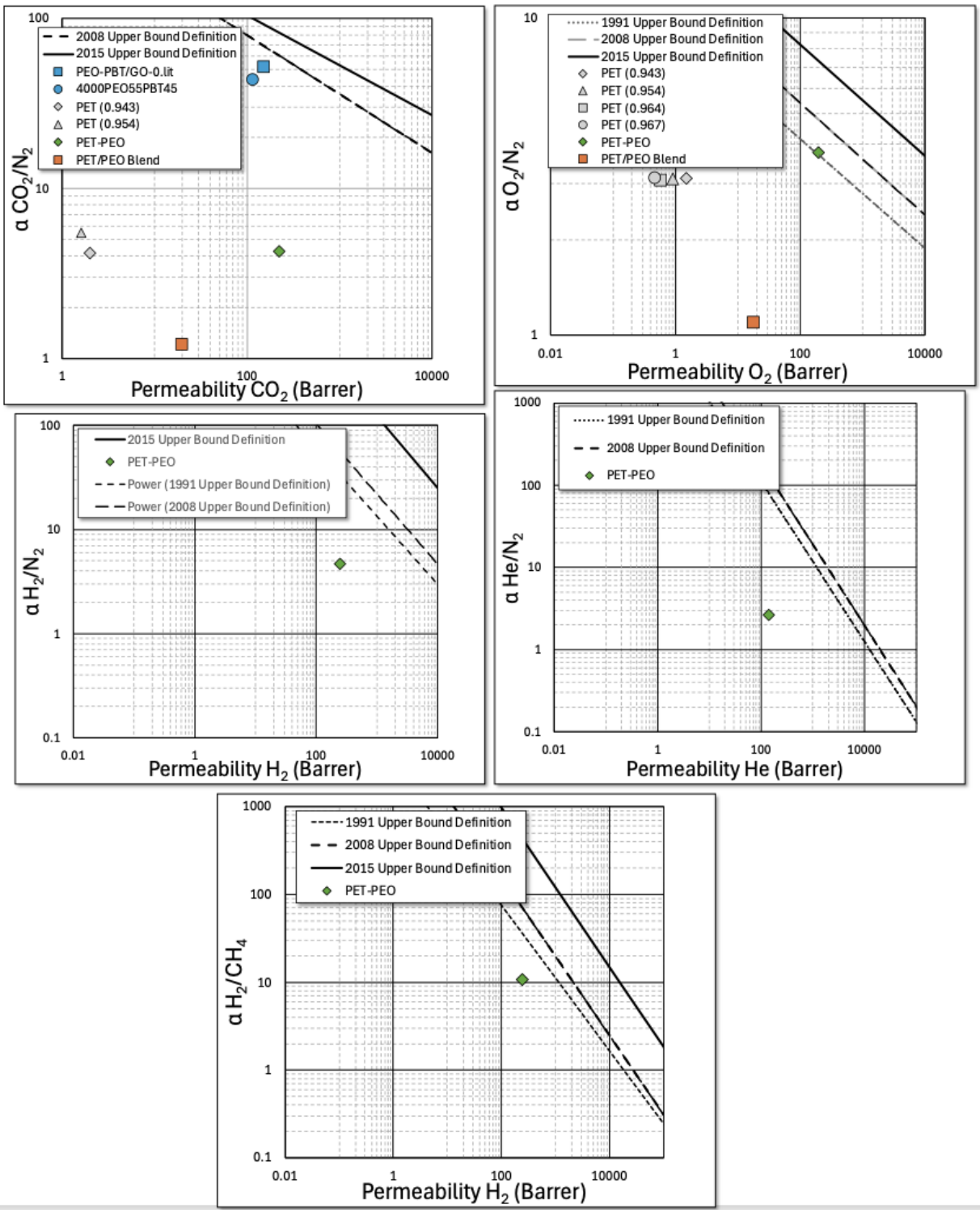

Figure S20 Robeson plots of gas permeability-selectivity performance for **(a)** CO_2/N_2 vs CO_2 permeability, **(b)** O_2/N_2 vs O_2 permeability, **(c)** H_2/N_2 vs H_2 permeability, **(d)** He/N_2 vs He permeability, and **(e)** H_2/CH_4 vs H_2 permeability, Literature data for PolyActive ($4000PEO_{55}PBT_{45}$[6] and PEO-PBT/GO-0[5]) and PET of varying densities are shown alongside experimentally measured short-end-capped PET-PEO multiblock copolymer (MBCP) and an 80:20 compatibilized

PET:PEO homopolymer blend (1 wt% compatibilizer) permeated with the corresponding gases. The 1991, 2008, and 2015 Robeson upper bounds are included as references.

To probe potential intermolecular interactions in the PET-PEO multiblock copolymer, FTIR spectra of PEO, virgin PET, rPET containing urethane linkages, and the PET-PEO MBCP were analyzed (**Figure S21**). In the 3200-3600 cm^{-1} region (**Figure S21c**), the MBCP exhibits a broadened absorption centered near ~3350 cm^{-1} relative to neat PEO, while rPET shows an even more pronounced broadening, consistent with hydrogen-bonded N-H and/or O-H stretching. Complementary changes are observed in the carbonyl region (1650-1760 cm^{-1}, **Figure S21b**), where the MBCP and rPET display peak broadening and a low-wavenumber shoulder relative to virgin PET, indicative of hydrogen-bonded carbonyl environments. Together, these features provide qualitative evidence for hydrogen-bonding interactions in the PET-PEO MBCP, likely arising from urethane N-H groups interacting with ester (PET) and ether (PEO) functionalities. While less pronounced than in the rPET sample, these interactions may contribute to intermolecular association within mixed amorphous regions and influence gas transport behavior.

Figure S21. FTIR spectra of PEO (4 kDa, blue), virgin PET (red), repolymerized PET (PET-HDI 1:1, green), and the PET-PEO multiblock copolymer (orange). **(a)** Full spectra **(b)** Carbonyl region

(1650-1760 cm^{-1}), where repolymerized PET and PET-PEO show broadened, lower-wavenumber features consistent with hydrogen-bonded carbonyls. **(c)** 3200-3600 cm^{-1} region, where repolymerized PET and PET-PEO exhibit broadened, red-shifted bands indicative of hydrogen-bonded N-H/O-H stretching in urethane-containing samples.

Polycarbonate Depolymerization

Figures S22 and **S23** illustrate the selective glycolysis of PC in the presence of both EG and BPA. As shown in **Figure S22**, EG promotes a more rapid depolymerization of PC than BPA, as evidenced by the faster, more pronounced decreases in both percent change in M_n and M_w in the EG-mediated reactions. Despite this higher depolymerization rate, the resulting products are not fully monomeric but instead consist primarily of PC oligomers bearing BPA end groups, in agreement with prior literature reports on PC glycolysis.[7] **Figure S23** further supports this assignment: the ^1H NMR spectra show the growth of methylene end-group resonances associated with BPA incorporation (**Figure S23b**), whereas the absence of methylene protons in the α-position of a hydroxyl end group associated with EG incorporation (**Figure S23c**) indicates the formation of phenol-terminated oligomers rather than extended ether-linked EG sequences. Together, these data confirm that EG-driven depolymerization yields a distribution of PC-BPA oligomers spanning a range of molar masses, enabling controlled tuning of oligomer size rather than complete breakdown to only small-molecule products.

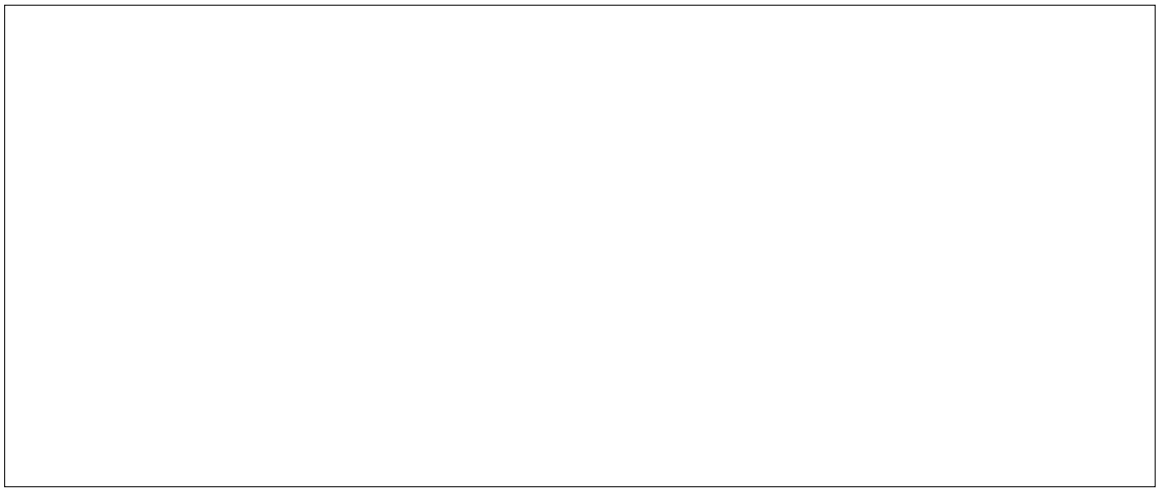

Figure S22 Percent change in molar mass determined by GPC for polycarbonate (PC) homogeneously depolymerized with ethylene glycol (EG, M_n grey line, M_w yellow line) and bisphenol-A (BPA, M_n blue line, M_w orange line).

Figure S23 (a) ^{1}H NMR spectra of PC and depolymerized PC samples, **(b)** showing the growth of the methylene end-group from depolymerization, and **(c)** showing no appearance of methylene protons in the alpha position, indicating a hydroxyl end group resulting from glycolysis of PC.

BPA-PEO Polymerization via diisocyanate coupling

Figures S24 and **Figure 7c**, together with **Table S6**, demonstrate the successful formation and growth of BPA-PEO multiblock structures via diisocyanate coupling. FTIR spectra in **Figure S24** show a gradual disappearance of the isocyanate stretching band over 0-4 h (highlighted in the pink region), concurrent with the emergence and growth of urethane carbonyl and N-H features (green region), confirming consumption of the HDI end groups and formation of urethane linkages between PEO and BPA. GPC traces in **Figure 7c** reveal progressive molar mass growth with reaction time following the initial short HDI end-capping step (10 min), consistent with step-growth coupling of PEO chains through BPA units.

Figure S24 FTIR of PEO-BPA polymerized via diisocyanate coupling, with PEO (blue), PEO-BPA 0 hour (orange), PEO-BPA 1 hour (green), PEO-BPA 2 hours (red), PEO-BPA 3 hours (purple), and PEO-BPA 4 hours (brown), highlighting the isocyanate group disappearing in the pink square and the urethane group forming with the green square.

The molar mass data in **Table S6** further quantify this evolution. The starting PEO ($M_n \approx$ 5.0 kDa, $Đ \approx 1.11$) is first converted to a low-molecular-weight, broad-dispersity PEO-BPA species at 0 h ($M_n \approx 1.5$ kDa, $Đ \approx 2.88$), reflecting the large difference in molar mass between the two blocks (PEO and BPA), and partial incorporation of BPA into the PEO chain. Continued reaction for 19 h produces a substantially higher molar mass PEO-BPA product ($M_n \approx 14.1$ kDa, $M_w \approx 22.6$ kDa) with a narrower dispersity ($Đ \approx 1.61$), indicative of efficient multiblock formation and chain growth. Collectively, **Figures S24, Figure 7c,** and **Table S6** confirm that diisocyanate-mediated coupling enables the synthesis of BPA-PEO multiblock architectures over a wide range of molar masses through controlled reaction time and extent of coupling.

Table S6 Molar mass and dispersity of PEO, PEO-BPA at 0 hours, and PEO-BPA at 19 hours.

Sample	M_n (kg/mol)	M_w (kg/mol)	Đ
PEO (4kDa)	5.0	5.6	1.1
PEO-BPA 0h	1.5	4.3	2.9
PEO-BPA 19h	14.1	22.6	1.6

PC-PEO polymerization via diisocyanate coupling

Figures S25, Figure 7d and **Table S7** further corroborate the successful formation of PC-PEO multiblock copolymers via diisocyanate coupling. FTIR spectra in **Figure S25** show the appearance of the isocyanate stretching band in the isocyanate-capped PC intermediate, which is absent in the starting PEO and subsequently consumed upon coupling to yield the PEO-PC product, consistent with urethane bond formation between PC-derived oligomers and PEO. GPC traces in **Figure 7d** reveal clear molar mass growth upon reaction, with the coupled PEO-PC sample at 19 h shifting to lower elution volumes relative to the starting 4 kDa PEO and depolymerized PC (dPC), indicating formation of higher-molecular-weight species as the coupling proceeds.

Figure S25 FTIR of PC-PEO polymerized via diisocyanate coupling, with PEO (blue), isocyanate-capped PC (orange), and PEO-PC (green). The isocyanate group is appearing in the isocyanate-capped PC sample.

Quantitative molar mass data in **Table S7** confirm this trend: PEO (M_n ≈ 5.0 kDa, Đ ≈ 1.11) and dPC (M_n ≈ 3.2 kDa, Đ ≈ 1.87) are converted into a higher-molecular-weight product after 48 h of coupling (M_n ≈ 8.0 kDa, Mw ≈ 15.7 kDa, Đ ≈ 1.96), reflecting step-growth assembly of telechelic oligomers into multiblock architectures. The broadened dispersity of the 19-h sample is consistent with this step-growth mechanism. DOSY NMR (**Figure S26**) further supports covalent incorporation of both components: the PEO and PC resonances in the PEO-PC product share a common diffusion coefficient that is distinct from those of the individual PEO and dPC precursors, indicating that both segments reside within a single diffusing macromolecular species. Together, **Figures S25, Figure 7d, Figure S26,** and **Table S7** provide a proof-of-concept demonstration that PC-derived oligomers can be effectively recombined with PEO via a unified

diisocyanate-coupling strategy to yield PC-PEO multiblock copolymers with increased molar mass and characteristic step-growth dispersity.

Table S7 Molar mass and dispersity of PEO, depolymerized PC (dPC), and PEO-BPA at 19 hours.

Sample	M_n (kg/mol)	M_w (kg/mol)	Đ
PEO	5.0	5.5	1.1
dPC	3.2	6.0	1.9
19h	8.0	15.7	2.0

Figure S26 DOSY NMR spectrum of (from left to right) the depolymerized PC, 4kDa PEO, and PEO-PC multiblock copolymer, showing coincident diffusion coefficients for PC and PEO resonances, consistent with covalent incorporation of both segments into a single diffusing species.

References

(1) Jehanno, C.; Flores, I.; Dove, A. P.; Müller, A. J.; Ruipérez, F.; Sardon, H. Organocatalysed depolymerisation of PET in a fully sustainable cycle using thermally stable protic ionic salt. *Green Chem.* **2018**, *20* (6), 1205-1212. DOI: 10.1039/c7gc03396f.
(2) Falkenstein, P.; Gräsing, D.; Bielytskyi, P.; Zimmermann, W.; Matysik, J.; Wei, R.; Song, C. UV Pretreatment Impairs the Enzymatic Degradation of Polyethylene Terephthalate. *Front. Microbiol.* **2020**, *11* (689), Original Research. DOI: 10.3389/fmicb.2020.00689.
(3) Watson-Sanders, S.; Dadmun, M. More Efficient Chemical Recycling of Poly(Ethylene Terephthalate) by Intercepting Intermediates. *ChemSusChem* **2024**, *17* (23). DOI: 10.1002/cssc.202301698.
(4) Watson-Sanders, S. R.; Johnson, K. D.; Taylor, T.; Barber, S.; Dadmun, M. D. Energy-Efficient Upcycling of Waste Poly(ethylene terephthalate) via Pre-Annealing-Induced Formation of Reactive Telechelic Oligomers. *ACS Sustain. Chem. Eng.* **2026**. DOI: 10.1021/acssuschemeng.5c12510.
(5) Karunakaran, M.; Shevate, R.; Kumar, M.; Peinemann, K. V. CO_2-selective PEO-PBT (PolyActive™)/graphene oxide composite membranes. *Chem. Commun.* **2015**, *51* (75), 14187-14190. DOI: 10.1039/c5cc04999g.
(6) Car, A.; Stropnik, C.; Yave, W.; Peinemann, K. V. Tailor-made Polymeric Membranes based on Segmented Block Copolymers for CO_2 Separation. *Adv. Funct. Mater.* **2008**, *18* (18), 2815-2823. DOI: 10.1002/adfm.200800436.
(7) Galan, N. J.; Dishner, I. T.; Sumpter, B. G.; Kertesz, V.; Abdul Rahman, N. B.; Polo-Garzon, F.; Demchuk, Z.; Saito, T.; Foster, J. C. Upcycling of polyethylene terephthalate to high-value chemicals by carbonate-interchange deconstruction. *Green Chem.* **2025**. DOI: 10.1039/d5gc03354c.